X-611-69-248
PREPRINT

NASA TM X-63583

2-20 KEV X-RAY SKY BACKGROUND

E. A. BOLDT
U. D. DESAI
S. S. HOLT
P. J. SERLEMITSOS

JUNE 1969

GSFC

GODDARD SPACE FLIGHT CENTER
GREENBELT, MARYLAND

2-20 KeV X-Ray Sky Background*

by

E. A. Boldt, U. D. Desai, S. S. Holt, and P. J. Serlemitsos

NASA/Goddard Space Flight Center
Greenbelt, Maryland 20771

ABSTRACT

The diffuse background of 2-20 keV x-rays over a band of the sky extending from Scorpius to the North galactic pole is found to be isotropic to within 5%, with a spectrum given by

$$10.3 \ E^{-n} \ \text{photons}/(\text{cm}^2\text{-sec-sr-keV}),$$

where $n = \left(1.35^{+0.07}_{-0.10}\right)$.

A comparison with spectra at higher energies indicates that the lower energy spectrum is flatter, corresponding to an apparent unit change in spectral index within the band 20-80 keV. A spectral break in this energy region has been discussed in connection with the collisional energy loss lifetime for metagalactic protons that radiate x-rays via inverse bremsstrahlung collisions with the ambient electrons of the intergalactic medium (Boldt and Serlemitsos 1969, Hayakawa 1969).

* Presented May 10, 1969 at Rome, Symposium No. 37 of the I.A.U., Non-Solar Gamma and X-Ray Astronomy.

2-20 KeV X-Ray Sky Background

by

E. A. Boldt, U. D. Desai, S. S. Holt, and P. J. Serlemitsos

NASA/Goddard Space Flight Center
Greenbelt, Maryland 20771

Observations of the diffuse x-ray background above approximately 20 keV, made from balloon platforms (Rothenflug et al., 1967, Agrawal et al., 1969, Bleeker 1969), indicate a spectral index for the photon flux of magnitude at least 2. Recent rocket observations (see review of Oda, 1969) of the background in a band extending down to about 1 keV suggest that the spectral index for this lower energy band is smaller than 2 and could be as low as 1.3. We report here on the results of a rocket flight launched from White Sands, New Mexico on March 3, 1969 in which we investigated the diffuse sky background within this band with a wide angle instrument especially suited to this purpose.

Figure 1 shows a schematic representation of the telescope, which consists of 6 argon-filled proportional counters of all-beryllium construction, enclosed in an anti- coincidence shield of plastic scintillator. All the counters were nominally identical except for the thin windows of the top counters which were of 2 mil beryllium. The pulses from these counters were in mutual anti-coincidence and the height of accepted pulses was analyzed by an on-board 128 channel analog to digital converter. We did not employ pulse shape discrimination.

A paddle mounted at the entrance of the telescope was rotated in discrete steps in order to vary the acceptance solid angle and thereby modulate a diffuse flux in a well-determined way. The telescope was contained in the rocket cylinder during the ascent and descent phases of the flight. During these phases the counters were calibrated with an Fe-55 source and the internal detector background spectrum was measured when the source was occulted by the paddle. The side door of the vehicle was opened at an altitude above 250,000 feet and the telescope was deployed in a direction normal to the vehicle axis. The first portion of the exposure was devoted to a measurement of Sco X-1 (see Holt et al., 1969). The second portion was a scan of about 1 degree per second along a great circle from Sco X-1 to an extended stop at the North galactic pole and provided the data for the results reported here. The count rate at mid-galactic latitudes was found to be within 5% of that measured at the North galactic pole.

The collimation angle in the scan direction is 14° FWHM, and 37° FWHM normal to it. The gross observed counting rate minus the measured detector background rate was verified to vary linearly with solid angle. Most genuine x-ray events occurred in the counters of the top layer, whereas extraneous background events induced by penetrating radiation in the environment occurred at the same rate in every counter, top or bottom. Figure 2 summarizes the modulating effect of the rotating paddle by exhibiting the observed counting rates per unit solid angle as a function of the solid angle of the telescope's field of view. We call attention to the lower graph of Figure 2 which shows the <u>net</u> counting rate per unit solid angle for the top counters to be independent of solid angle and indicates that the events from these counters used for the primary spectral analysis are due entirely to a diffuse flux of x-rays.

In order to evaluate the spectrum of the incident flux we assumed a power law for a range of spectral indices and folded these hypothetical spectra through the measured response functions of our detectors. After a normalization to the total count, the expected spectra were compared with the observations over intervals that are 4 channels wide, which amount to increments of about 1 keV. The single hypothesis that fits best for <u>all</u> three top counters is shown in Figure 3. The three histograms result from the same assumed incident spectrum as folded through the slightly different response functions measured for the three top counters A1, A2 and A3. The observed data are shown by diamonds. The χ^2 evaluation of these results indicates a good statistical fit for each of these counters taken separately as well as for all taken together.

We find limits 1.25 and 1.42 on the spectral index. These limits correspond to hypotheses that yield values of χ^2 within a 68% probability band centered about the most probable value. From the point of view of statistics, these results essentially rule out an index larger than 1.6.

In order to examine systematic errors in this spectral determination, we compared the normalizations obtained independently from the top and bottom counters. Since the bottom and top counters are internally identical, and since the flux traversing the top counters and entering the bottom counters is spectrally hardened, such a comparison constitutes a severe test for systematic errors. We assume incident spectra of the form CE^{-n}, fold them through the response functions of the counters, and normalize to the observed count in the range 2-20 keV. Figure 4 shows the results of this analysis; we plot here the ratio of C obtained from the top counters to C obtained from the bottom counters for various assumed values of the spectral index (n) of the incident diffuse flux. If there were perfect precision in our measurement of the relative efficiencies of the top and bottom counters, then the value of the spectral index n that yields a ratio of unity would definitely be the appropriate one. However, the precision in our relative calibration is 3% and is shown by dotted lines. Considering all limits, this comparison constrains acceptable values of the spectral index to be within 1.4 and 1.5. Therefore, we conclude that the evidence presented here is sufficiently free of systematic as well as statistical errors to give a strong indication that the index is in fact close to 1.4. These results are in good agreement with those obtained above 1.5 keV by Henry et al., (1968) for the North galactic pole region and with those obtained for the anti-center of the galaxy by Ducros et al., (1969) as well as by us in a previous experiment (Boldt et al., 1969).

In summary, our results give a spectrum for the diffuse background over the band 2-20 keV as

$$10.3\ E^{-n}\ \text{photons}/(\text{cm}^2\text{-sec-sr-keV}),$$

where E is the photon energy in keV, and $n = (1.35\ ^{+0.07}_{-0.10})$.

The value of the normalization constant (C) is determined from an absolute calibration of the detection efficiency of the telescope to a broad beam of x-rays of known intensity at 14.4 keV (Co-57) and 22.3 keV (Cd-109) from distant on-axis radio-active sources. The geometry factor required for a diffuse flux measurement involves knowing this efficiency at all angles. We have calculated this from the measured normal broad beam response on the basis of a detailed, but necessarily approximate, evaluation of our relatively complicated detector geometry. The OSO III satellite observations of hard diffuse x-rays with a NaI scintillation detector by Schwartz et al., (1969) extend down into our spectral region and overlap in energy with our observations for their bands 7.7-12.5 keV and 12.5-22 keV. The flux values observed by the scintillator are about 30% lower than would be expected for each of these two bands on the basis of our power law spectrum. This discrepancy is indicative of the magnitude of systematic errors made in determining the absolute detection efficiency for a diffuse x-ray flux at these energies.

A spectral picture that emerges is one where the band 2-20 keV ($\bar{E} \approx 6$ keV) may be described with $n \approx 1.4$, whereas $n \approx 2.0$-2.4 (Agrawal et al., 1969, Rothenflug et al., 1967) may be required for the band 20-80 keV ($\bar{E} \approx 36$ keV), and $n \approx 2.5$ (Bleeker, 1969) for the band 20-220 keV ($\bar{E} \approx 43$ keV). An intermediate energy band 4-40 keV ($\bar{E} \approx 10$ keV) has been studied from a rocket observation (Seward et al., 1967) and may be described with $n \approx 1.6$, an intermediate value for the spectral index. Taken together, all these results suggest a change in spectral index of about unity within the interval 20-80 keV.

A possible unit change in the spectral index has been attributed by Henry et al., (1968) to a hypothetical break at >1 GeV in the spectrum of metagalactic electrons generating x-rays via inverse Compton scattering with ambient low energy photons. If we are dealing with bremsstrahlung x-rays, then the electron spectrum would have to break at $\gtrsim$ 20 keV (Silk and McCray, 1969). However, as pointed out by Boldt and Serlemitsos (1969) and emphasized at this meeting by Hayakawa (1969), the inverse bremsstrahlung of suprathermal protons with the ambient electrons of the intergalactic medium probably provides the only natural set of circumstances for a spectral break in the correct energy region. A break in the proton spectrum at 40 MeV would give a corresponding break in the inverse bremsstrahlung x-rays at 20 keV (Boldt and Serlemitsos, 1969); a 40 MeV proton has a lifetime of about 10^{10} years for collisional energy loss in a medium of 10^{-5} electrons/cm^3, and therefore exhibits a feature that is sufficient to provide the required spectral break for metagalactic protons.

It is a pleasure to thank Messrs. F. Birsa, R. Bleach, M. Ziegler and the rocket instrumentation and operating crews at the Goddard Space Flight Center and at the White Sands Missile Range for their important contributions to the success of this experiment.

References

Agrawal, P. C., Appa Rao, M. V. K., Biswas, S., Gokhale, G. S., Iyenger, V. S., Kunte, P. K., Manchanda, R. K., and Sreekantan, B. V., 1969, Symposium No. 37 of I. A. U., Non-Solar Gamma and X-Ray Astronomy, Rome (to be published).

Bleeker, J. A. M., 1969, Symposium No. 37 of I. A. U., Non-Solar Gamma and X-Ray Astronomy, Rome (to be published).

Boldt, E. A., Desai, U. D., and Holt, S. S., 1969, Ap. J. 156, 427.

Boldt, E. and Serlemitsos, P., 1969, Ap. J. 157 (in press).

Ducros, G., Ducros, R., Rocchia, R., and Tarrius, A., 1969, (preprint) C. E. N., Saclay, France.

Hayakawa, S., 1969, Symposium No. 37 of I. A. U., Non-Solar Gamma and X-Ray Astronomy, Rome (to be published).

Henry, R. C., Fritz, G., Meekins, J. F., Friedman, H., and Byram, E. T., 1968, Ap. J. (Letters), 153, L 11.

Holt, S. S., Boldt, E. A., and Serlemitsos, P. J., 1969, Symposium No. 37 of I. A. U., Non-Solar Gamma and X-Ray Astronomy, Rome (to be published).

Oda, M., 1969, Symposium No. 37 of I. A. U., Non-Solar Gamma and X-Ray Astronomy, Rome (to be published).

Rothenflug, R., Rocchia, R., Boclet, D., and Durouchoux, P., 1967, Space Research VII, (Amsterdam: North Holland Publishing Co.)

Schwartz, D. A., Hudson, H. S., and Peterson, L. E., 1969 (private communication).

Seward, F., Chodil, G., Mark, H., Swift, C., and Toor, A., 1967, Ap. J. 150, 845.

Silk, J. and McCray, P., 1969 (preprint).

Figure Captions

Figure 1. Schematic diagram of the x-ray telescope. The proportional counters are 2" x 2" x 6", filled with a P-10 Argon-Methane gas mixture at atmospheric pressure. A multilayer graded (Sn-Cu-Al) shield surrounds the plastic scintillator. A stepping motor rotates the paddle through 36° every 2.6 seconds.

Figure 2. The observed counting rate per unit solid angle as a function of the solid angle of the telescope. The lower graph is for the composite of the three top counters; the net rate is derived from the gross rate by subtracting the detector background measured when the telescope was enclosed within the rocket cylinder. The top graph is for the composite of all six counters, top and bottom. Each dotted line is at the level of the average counting rate for the five data points of the set considered. The five data points of each set correspond to the five distinguishable positions of the paddle. Note that the four sets of such points exhibited here are <u>not</u> statistically independent sets since there is overlap of data among these four categories.

Figure 3. The observed counts per second (diamonds) for each of the top counters (A1, A2, A3) as a function of the detected energy (keV). The three histograms are the result of folding the indicated incident flux through the measured

response function of each detector.

Figure 4. The ratio of the normalization constant (C) obtained from the top counters to (C) obtained from the bottom counters is shown for several assumed values for the spectral index (n) of the incident diffuse flux. The dispersions for these points correspond to rms deviations among the values obtained from the counters of each level.

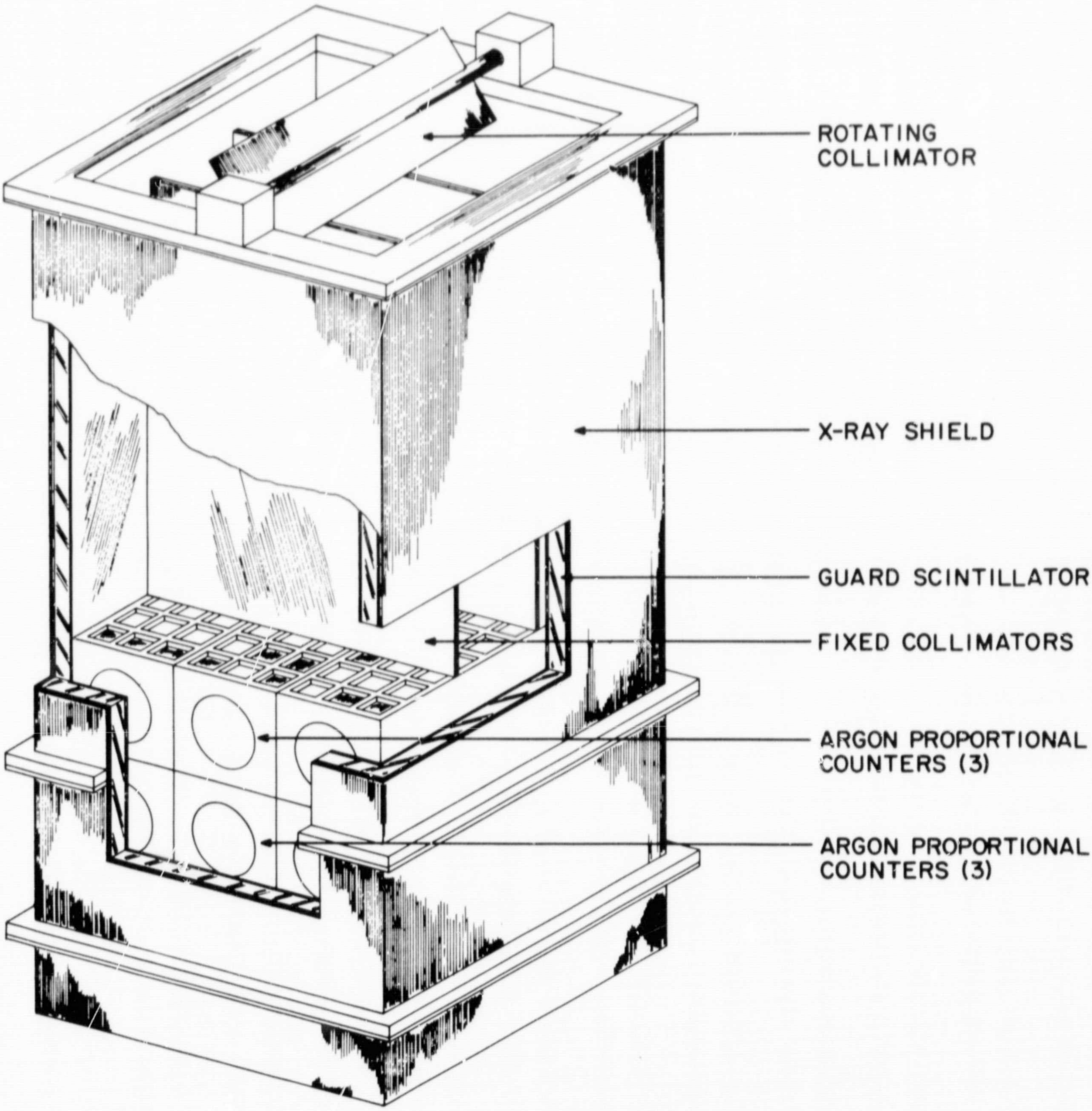

SCHEMATIC DIAGRAM OF X-RAY DETECTOR

Figure 1

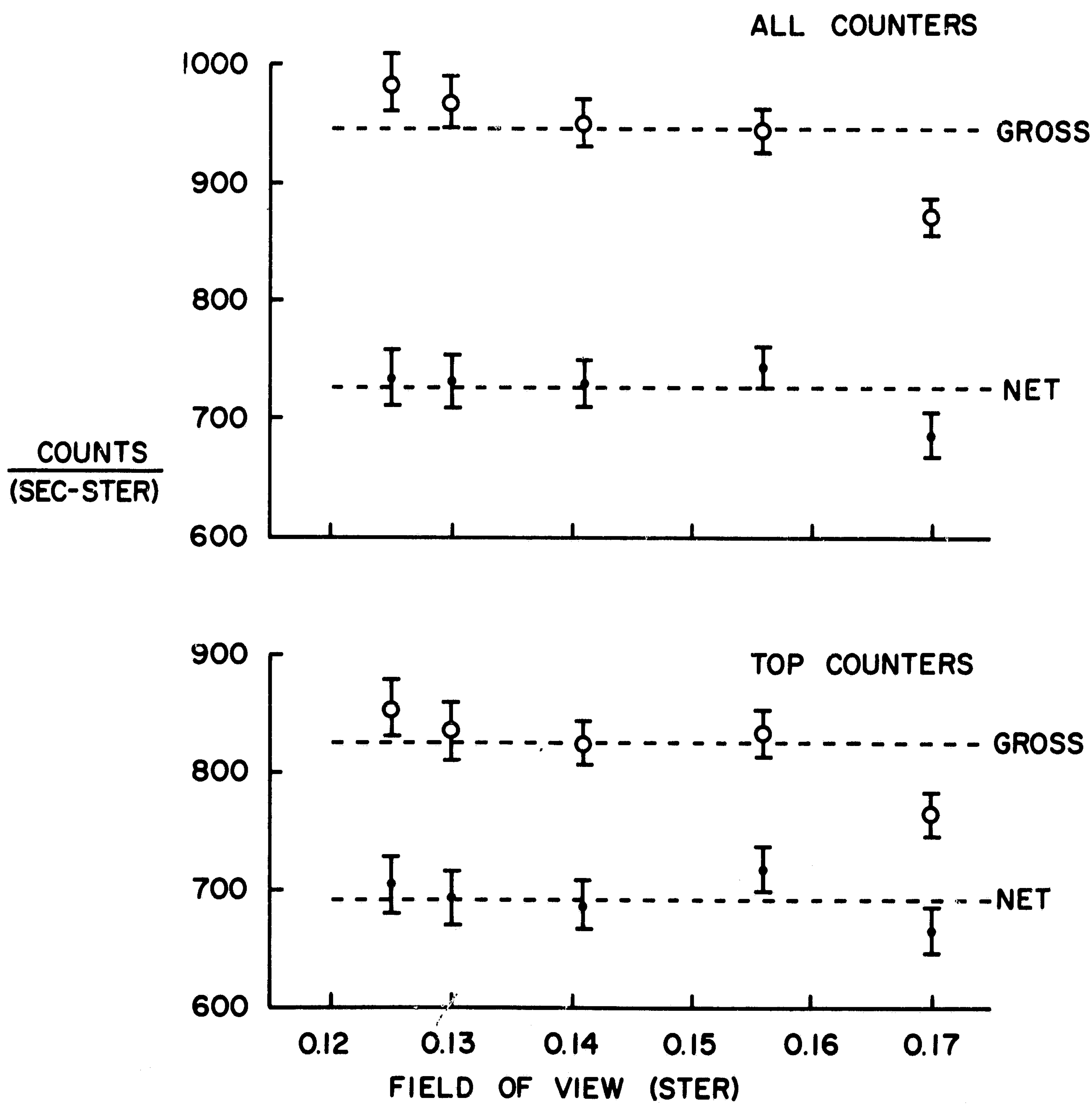
ALL COUNTERS
GROSS
NET
1000
900
800
700
600
COUNTS
(SEC-STER)
TOP COUNTERS
GROSS
NET
900
800
700
600
0.12
0.13
0.14
0.15
0.16
0.17
FIELD OF VIEW (STER)

Figure 2

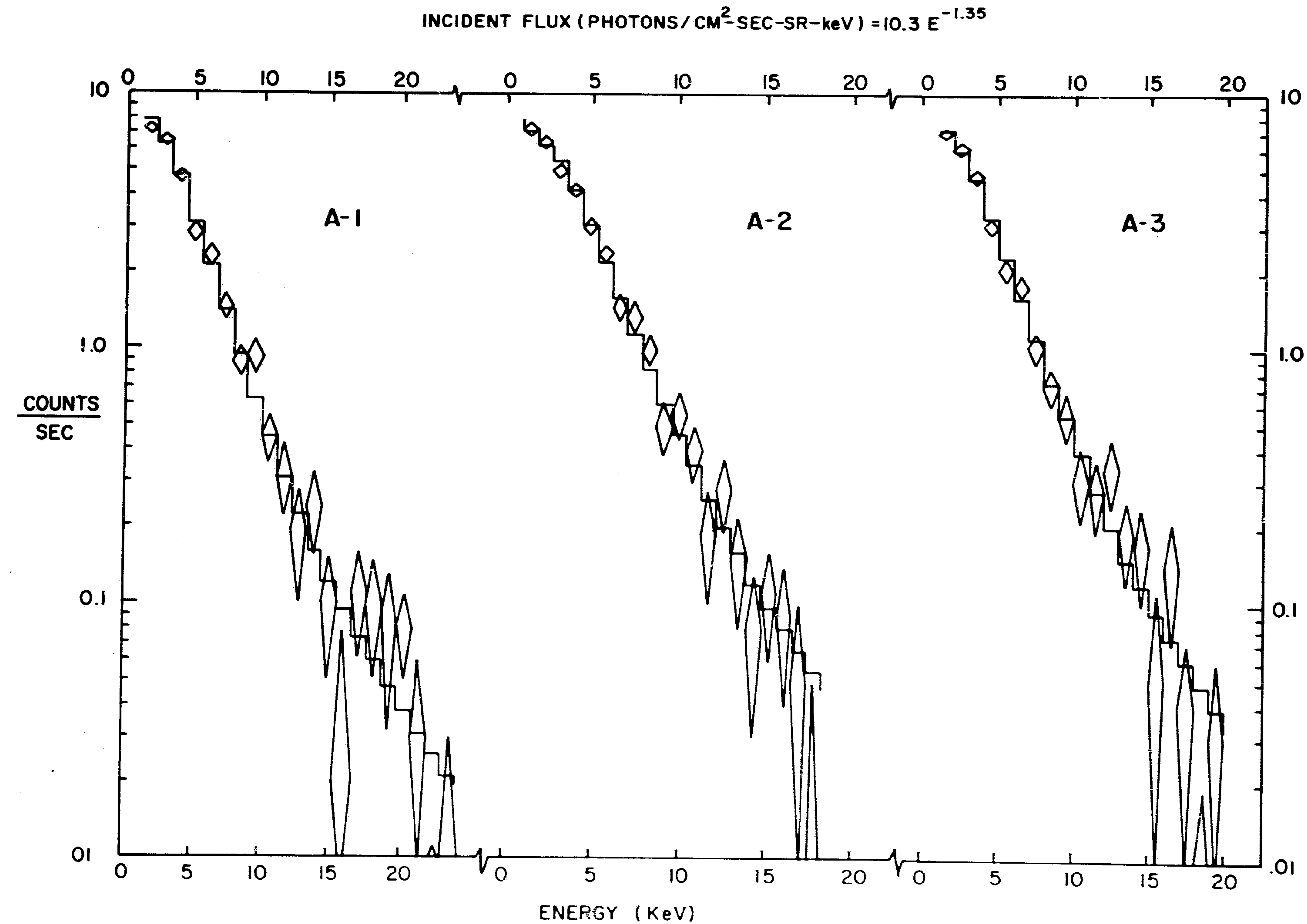

INCIDENT FLUX (PHOTONS/CM^2-SEC-SR-keV) = 10.3 E$^{-1.35}$
COUNTS / SEC
A-1
A-2
A-3
ENERGY (KeV)

Figure 3

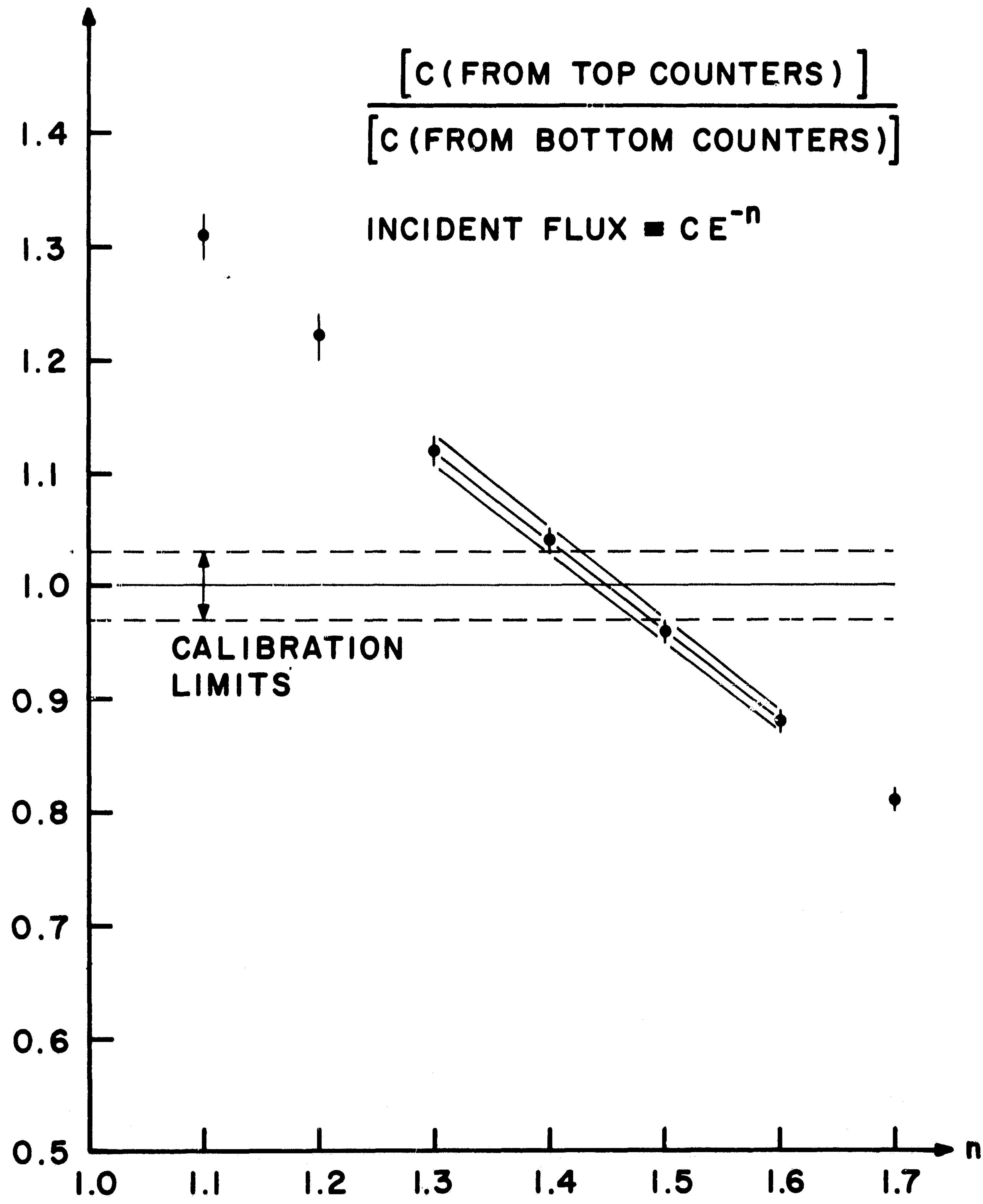

[C(FROM TOP COUNTERS)]
[C(FROM BOTTOM COUNTERS)]
INCIDENT FLUX = C E^-n
CALIBRATION LIMITS
1.4
1.3
1.2
1.1
1.0
0.9
0.8
0.7
0.6
0.5
1.0
1.1
1.2
1.3
1.4
1.5
1.6
1.7
n

Figure 4